Rapid Communications

Higher-order topological insulators protected by inversion and rotoinversion symmetries

Guido van Miert[1] and Carmine Ortix[1,2]

[1]*Institute for Theoretical Physics, Center for Extreme Matter and Emergent Phenomena, Utrecht University, Princetonplein 5, NL-3584 CC Utrecht, Netherlands*

[2]*Dipartimento di Fisica "E. R. Caianiello", Universitá di Salerno, IT-84084 Fisciano, Italy*

(Received 21 June 2018; published 13 August 2018)

We provide the bulk topological invariant for chiral higher-order topological insulators in (i) fourfold rotoinversion invariant bulk crystals, and (ii) inversion-symmetric systems with or without an additional threefold rotation symmetry. These states of matter are characterized by a nontrivial $\mathbb{Z}_2$ index, which we define in terms of symmetric hybrid Wannier functions of the filled bands, and can be readily calculated from the knowledge of the crystalline symmetry labels of the bulk band structure. The topological invariant determines the generic presence or absence of protected chiral gapless one-dimensional modes localized at the hinges between conventional gapped surfaces.

DOI: 10.1103/PhysRevB.98.081110

Introduction. Free electrons in a crystal can be universally described in terms of Bloch waves. In ordinary band insulators, however, electronic states can be equivalently represented using exponentially localized Wannier functions (WFs), i.e., the Fourier transform of the Bloch waves up to a unitary basis transformation. When (non)spatial symmetries are involved, this gauge degree of freedom can be exploited to construct WFs respecting the set of symmetries characterizing the insulating crystal [1–3]. Symmetry-protected topological (SPT) insulators do not allow for such a Wannier representation. This is because the most generic SPT cannot be adiabatically deformed to a trivial atomic insulator [4,5], whose orbitals naturally form a set of symmetric WFs. Henceforth, the presence of "anomalous" gapless boundary states [6,7]—the prime physical consequence of a bulk nontrivial topology—can be related to an obstruction in representing the ground state of the system in terms of symmetric WFs [5,8].

Nevertheless, a description of a SPT state in terms of symmetric hybrid Wannier functions (HWFs), the partial Fourier transform of Bloch waves, is entirely allowed [9]. An inversion-symmetric Chern insulator, for instance, can be described using HWFs obeying the property $w_k^{\text{hybrid}}(x) \equiv w_{-k}^{\text{hybrid}}(-x)$. At the two momenta $k = 0, \pi$ the HWFs thus correspond to inversion-symmetric one-dimensional (1D) WFs whose charge centers constitute a genuine topological invariant [10], and dictate the existence of quantized end charges in open geometries [11–13]. These effective 1D crystalline topologies are not only interesting *per se*. In fact, and as shown below, their mismatch allows, in a very simple manner, to diagnose the parity of the integer Chern number characterizing the two-dimensional topological insulating state.

Starting out from this observation, in this Rapid Communication we define the bulk topology of second-order topological insulators [14–24]—crystalline systems with gapped $(d-1)$ surface states but gapless $(d-2)$ chiral hinge modes—protected only by spatial inversion and rotoinversion symmetries. To this end, we will first define the crystalline topology of rotationally symmetric two-dimensional (2D) insulators with zero Chern number using symmetric WFs. The corresponding topological invariants, which can be also expressed in terms of the symmetry labels in the band-structure representation [25,26], directly pinpoint the presence of quantized corner charges in open geometries [27–33]. Thereafter, we will show that a mismatch between these 2D crystalline topological invariants in the symmetric HWF representation of a bulk three-dimensional crystal, encoded in a $\mathbb{Z}_2$ topological invariant, dictates the existence of protected chiral hinge modes. In the remainder, we present explicit calculations for fourfold rotoinversion-symmetric crystals and refer to the Supplemental Material [34] for other point-group symmetries.

Crystalline topology of 2D insulators via symmetric WFs. We first recall the concept of Wyckoff positions. General positions in the unit cell can be classified into a few types of Wyckoff positions depending upon their site symmetry group. In particular, for a two-dimensional crystal with $\mathcal{C}_4$ rotational symmetry, there are two Wyckoff positions that are invariant under fourfold rotation [cf. Fig. 1(a)], which can be fixed at the origin $\mathbf{r} = \{0, 0\}$ (A) and at the corner of the unit cell $\mathbf{r} = \{1/2, 1/2\}$ (C). The two sites $\mathbf{r} = \{1/2, 0\}$ (B) and $\mathbf{r} = \{0, 1/2\}$ (D) are instead separately invariant under twofold rotations, but are transformed into each other by a fourfold rotation. This also implies that symmetric WFs centered at the Wyckoff positions A, C are classified [34] by the rotation eigenvalues ± 1, $\pm i$, whereas symmetric WFs locating at B, D are specified by the twofold rotation eigenvalues ± 1. Henceforth, the ground state of an atomic insulator in a $\mathcal{C}_4$-symmetric crystal can be characterized by a set of ten integers [35] $N_{W;r}$, each of which denotes the number of occupied symmetric WFs located at site W with rotation eigenvalue r. However, this set of integers does not yield a $\mathbb{Z}^{10}$ topological classification, since, taken separately, the integers $N_{W;r}$ do not represent genuine topological invariants.

We illustrate this by considering a paradigmatic tight-binding model [see Fig. 1(a)] with four atomic sites in the unit cell at full filling. Considering first the longer-range hopping amplitudes $t_{2,3}$ to be much smaller than the nearest-neighbor

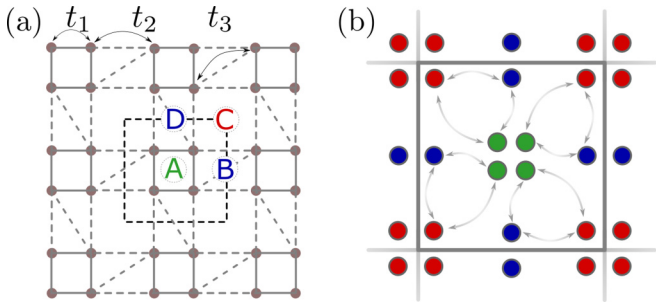

FIG. 1. (a) A tight-binding model for a $\mathcal{C}_4$-symmetric crystal with four atoms in the unit cell. We explicitly indicate the hopping amplitudes and the Wyckoff positions in the unit cell. (b) Three topologically equivalent orbital configurations with different sets of $N_{W;r}$ integers.

hopping t_1, the system can be described in terms of four WFs centered at the Wyckoff position A, which yields $N_{A;\pm1,\pm i} \equiv 1$ while $N_{B;\pm1} \equiv N_{C;\pm1,\pm i} \equiv 0$. However, by continuously increasing the diagonal hopping t_3, the system can be more conveniently described in terms of four symmetric WFs centered at the Wyckoff position C, thus implying $N_{C;\pm1,\pm i} \equiv 1$ and $N_{B;\pm1} \equiv N_{A;\pm1,\pm i} \equiv 0$. Likewise, in the $t_2 \gg t_{1,3}$ regime the system can be described in terms of symmetric WFs centered at the twofold symmetric Wyckoff positions B and D, in which case $N_{A;\pm1,\pm i} \equiv N_{C;\pm1,\pm i} \equiv 0$ while $N_{B;\pm1} \equiv N_{D;\pm1} \equiv 1$. Since these continuous deformations in the hopping patterns do not change the topology of the insulating state, we find that the three configurations in Fig. 1(b) are all equivalent.

To proceed further, we therefore define a subset of integers demanding their topological "immunity" against such continuous deformations. Since the latter simply correspond to $N_{W;r} \to N_{W;r} \pm 1 \; \forall \, r$, we are led to define a new set of seven integers explicitly reading

$$\nu_{W;\bar{r}} = -3N_{W;\bar{r}} + \sum_{r\neq\bar{r}} N_{W;r}, \quad \bar{r} = \pm1, i, \quad W = A, C,$$
$$\nu_B = -N_{B;1} + N_{B;-1}. \tag{1}$$

The reduced $\mathbb{Z}^7$ topological classification predicted by this integer set is in perfect agreement with the band-structure combinatoric approach of Ref. [26], where the topological invariants are related to the multiplicities Γ_r, M_r, and X_r of the fourfold and twofold rotation eigenvalues r at the high-symmetry (HS) points in the Brillouin zone [36]. This motivates us to find a one-to-one correspondence between the real-space invariants listed in Eq. (1) and the rotation-symmetry labels of the band structure. It has a dual purpose: First, it proves that a change in the integers reported in Eq. (1) is necessarily accompanied by a bulk gap closing and reopening; second, it allows one to bypass the problem of constructing symmetric WFs. In particular, we obtain the following relations (see Ref. [34] for the other invariants):

$$\nu_{A;1} = -3\Gamma_1 - \Gamma_{-1} + 2M_{-1} + X_{-1} + \frac{3}{2}[M_{-i} + M_i - \Gamma_i - \Gamma_{-i}],$$

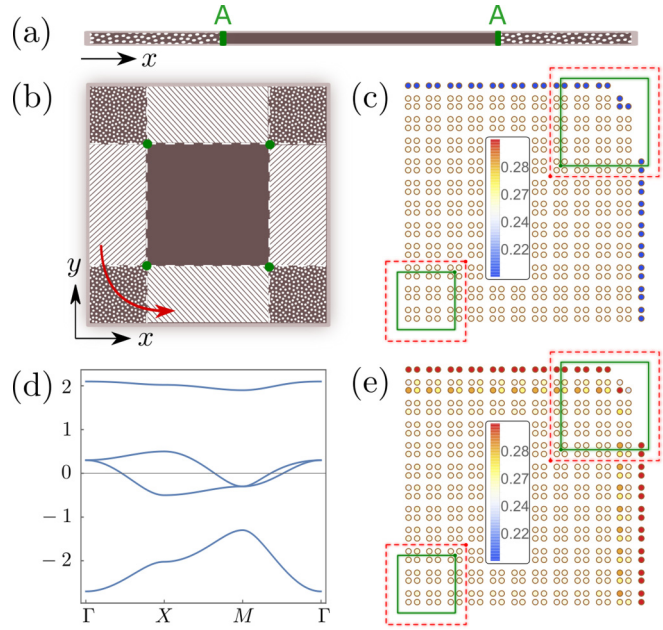

FIG. 2. Sketch of (a) a finite inversion-symmetric 1D chain and (b) a finite $\mathcal{C}_4$-symmetric 2D crystal. (c) Local charge distribution at quarter filling for the model shown in Fig. 1(a) with $t_1 = 1$, $t_2 = t_3 = 0$, and $E_F = -1.8$. (d) Bulk band structure for $t_1 = 1$, $t_2 = 0.2$, and $t_3 = 0.3$. Here, $\Gamma = (0, 0)$, $M = (\pi, \pi)$, and $X = (\pi, 0)$. (e) Corresponding local charge distribution with $E_F = -0.8$. The charge inside the red dashed (green solid) squares corresponds to Q_A (Q_C).

$$\nu_{C;1} = 2[\Gamma_{-1} - M_{-1}] - X_{-1} + \frac{3}{2}[\Gamma_i + \Gamma_{-i}] - \frac{M_i + M_{-i}}{2},$$
$$\nu_B = \frac{1}{2}[\Gamma_i + \Gamma_{-i} - M_i - M_{-i}]. \tag{2}$$

Corner charges. Having established the $\mathbb{Z}^7$ topological classification of $\mathcal{C}_4$-symmetric crystals solely by virtue of symmetric WFs, we next show how this crystalline topology can be probed in systems with open geometries. We first recall that in a inversion-symmetric insulating finite atomic chain, the excess left (right) edge charge, defined as the fractional part of the total charge measured from $-\infty$ ($+\infty$) up to some reference point located sufficiently far away from the edges, is quantized to 0 or 1/2 if the reference point coincides with one of the two inversion centers of the chain [cf. Fig. 2(a)]. This is because the excess left Q_A^L and right Q_A^R edge charges must be identical due to inversion symmetry. In addition, the total bulk charge contained between the two inversion reference centers must be an integer, which therefore implies $2Q_A^L = 2Q_A^R = 0 \bmod 1$. Moreover (see Ref. [34]), the half-integer value of the excess end charge can be immediately related to the $\mathbb{Z}_2$ part of the integer crystalline topological invariant for an inversion-symmetric insulating atomic chain.

Now we show that a very similar result holds for the corner charge of a $\mathcal{C}_4$-symmetric insulator. Let us consider the square geometry shown in Fig. 2(b) with four symmetry-related corners, and define the corner charge Q_A as the fractional part of the charge contained in the region $(-\infty, j] \times (-\infty, j]$, with j a sufficiently large integer. This automatically constrains the

reference point to coincide with a Wyckoff position A. Q_A can be dubbed a "topological" bulk quantity if and only if its quantized value is insensitive to the microscopic details both at the corners and at the edges. The former condition is immediately verified if we concomitantly assume both the bulk and the edges to be completely insulating. To investigate the insensitivity to microscopic details at the edge, we consider the situation in which an edge potential is applied to, e.g., the lower edge in Fig. 2(b). The induced charge flow from the corner to the edges, or vice versa, will result in a loss of quantization of the corner charge Q_A. However, if the applied edge potentials respect the fourfold rotational symmetry of the bulk crystal, the charge flow induced by the lower edge will be precisely compensated by the charge flow due to the left edge. Hence, the fourfold rotational symmetry of the crystal guarantees the bulk nature of the corner charge. The discretization of its value can be read off by considering that $4Q_A + 4Q_{\text{edge}} = 0 \bmod 1$, where Q_{edge} represents the edge charge contained in the dashed region of Fig. 2(b). Since the latter is quantized to half-integer values [13], we find that the corner charge assumes values discretized in multiples of $1/4$ modulo an integer. More importantly, we can immediately relate the corner charge to the formerly defined $\mathbb{Z}$ integer invariants using that $Q_A = \sum_r N_{A;r}/4 \equiv \nu_{A;\bar{r}}/4$ modulo an integer $\forall\, \bar{r}$. These relations can be rationalized by considering that for a fourfold rotational-symmetric insulator in the atomic limit, i.e., where all hopping amplitudes connecting atomic sites are set to zero, the fractional part of the corner charge comes only about WFs centered at the reference point $\{j, j\}$, each of which contributes with a quarter of the electronic charge. By invoking the principle of adiabatic continuity, this result holds also when switching on the hopping amplitudes provided the band gap does not close and reopen. A similar analysis can be performed for the corner charge with a reference point $\{j + 1/2, j + 1/2\}$ corresponding to a Wyckoff position C. Moreover, for corners where the reference point is chosen at the twofold rotational-symmetric Wyckoff positions B and D, it is possible to show that the sum of the charge contained in two corner partners is quantized in multiples of half of the electronic charge [34]. All in all, we therefore find that corner charges are able to probe a $\mathbb{Z}_4 \otimes \mathbb{Z}_4 \otimes \mathbb{Z}_2$ part of the general $\mathbb{Z}^7$ crystalline topology.

To corroborate our findings, we next present explicit calculations for the tight-binding model shown in Fig. 1(a). Figure 2(c) shows the charge distribution at one-quarter filling setting the hopping amplitudes $t_2 \equiv t_3 \equiv 0$. In this case the system consists of uncoupled molecules centered at Wyckoff position A. Consequently, the bulk band structure is made out of flatbands with energies ± 2 and 0. For the regular lower left corner in Fig. 2(c) visual inspection immediately reveals that the corner charge $Q_A = 1/4$ while $Q_C = 0$, which is in perfect agreement with the fact that $\nu_{A;\bar{r}} = 1 \bmod 4$ and $\nu_{C;\bar{r}} = 0 \bmod 4$. Notice that these values of the corner charges are insensitive to the specific termination as long as the edges are related by the fourfold symmetry [cf. the upper right corner in Fig. 2(c)]. More importantly, the quantization of the corner charge is preserved even for $t_2 \neq t_3 \neq 0$, in which case the bulk band acquires a full dispersion [cf. Fig. 2(d)] and the electronic charge density in the corner region is manifestly inhomogeneous [cf. Fig. 2(e)].

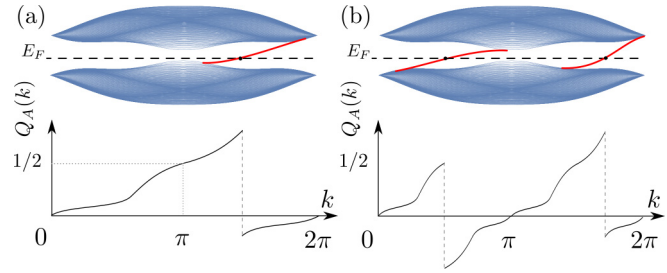

FIG. 3. End-charge flow patterns for inversion-symmetric (a) odd- and (b) even-integer Chern insulators. In both cases, the edge charge is an odd function in the momentum k up to integer jumps.

Chiral hinge states in rotoinversion-symmetric crystals. Next, we show how the topological invariants underpinning the presence of quantized corner charges can be used to define the bulk $\mathbb{Z}_2$ topological invariant of a second-order topological insulator. Let us first consider the aforementioned example of a two-dimensional Chern insulating state in an inversion-symmetric crystal put in a ribbon geometry. Assuming the translational symmetry to be preserved in the $\hat{x}$ direction, one can view the full system as a collection of one-dimensional finite chains with the momentum k_x playing the role of an external parameter. Inversion symmetry of the two-dimensional crystal implies that the right edge charge at k_x is identical to the left edge charge at $-k_x$. This, in turns, implies the constraint for the single edge charge $Q_A(k_x) = -Q_A(-k_x) \bmod 1$, i.e., $Q_A(k_x)$ is an odd function up to integer jumps, which correspond to edge states crossing the Fermi level E_F. Moreover, this guarantees the quantization of the edge charge along the inversion-symmetric lines $k_x = 0, \pi$. With these relations, we can identify two "topologically" distinct states of the original two-dimensional crystal. In fact, for $Q_A(0) - Q_A(\pi) = 1/2 \bmod 1$ an odd number of in-gap states must cross the Fermi level at each edge [cf. Fig. 3(a)] during an adiabatic cycle of $k_x \in [0, 2\pi]$. On the contrary, an even number of in-gap states will cross the Fermi level for $Q_A(0) - Q_A(\pi) = 0 \bmod 1$ [cf. Fig. 3(b)]. As a result, we find that the crystalline topology of the two inversion-symmetric chains at $k_x = 0, \pi$ is able to diagnose the Chern number parity of the 2D crystal.

Let us now exploit a similar connection for the quantized corner charges and consider a three-dimensional crystal with a fourfold rotoinversion symmetry (see Ref. [34] for other point-group symmetries) $\mathcal{S}_4 = \mathcal{C}_4 \times \mathcal{M}_z$, where $\mathcal{M}_z$ indicates the mirror symmetry in the $\hat{z}$ direction. As before, we consider the bulk three-dimensional Hamiltonian as a collection of two-dimensional Hamiltonians $\mathcal{H}(k_z)$ parametrized by the momenum k_z. The fourfold rotoinversion symmetry immediately implies that the two-dimensional Hamiltonians $\mathcal{H}(0), \mathcal{H}(\pi)$ both inherit the fourfold rotoinversion symmetry $\mathcal{S}_4$. Therefore, the three-dimensional crystal can be classified topologically by $\mathbb{Z}^{14}$ [37]. These 14 invariants, however, are not all independent when requiring a full bulk band gap. This is due to the fact that the collection of two-dimensional Hamiltonians all possess a twofold rotational symmetry $\mathcal{C}_2 = (\mathcal{S}_4)^2$. In order to prevent band-gap closing along the HS lines $(0, 0, k_z)$, $(\pi, 0, k_z)$, $(0, \pi, k_z)$, and (π, π, k_z), the multiplicities of the twofold rotational symmetry eigenvalues must therefore remain constant.

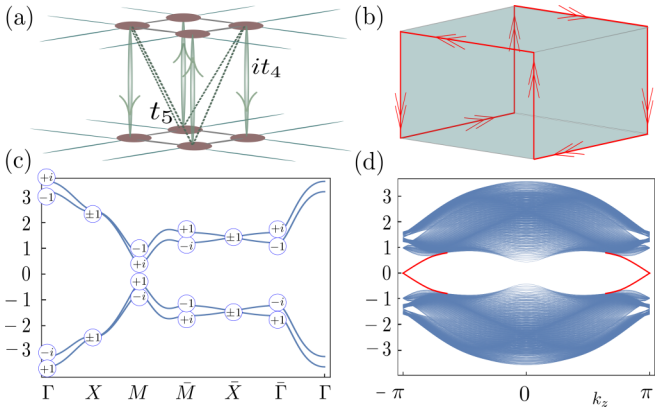

FIG. 4. (a) Closeup of the 3D crystal. (b) Chiral hinge state pattern in a nontrivial $\mathcal{S}_4$-symmetric insulator. (c) Bulk band structure along HS lines, with the corresponding symmetry labels. HS points with (without) the bar lie in the $k_z = \pi$ ($k_z = 0$) plane. Here, we have used $t_1 = t_5 = 0.7$, $t_2 = 1$, $t_3 = 0.2$, and $t_4 = 0.5$. (d) Band structure with periodic boundary conditions in the $\hat{z}$ directions and open in the $\hat{x}$ and $\hat{y}$ directions.

These four constraints imply that the two-dimensional topological crystalline integer invariants $\nu_{A(C);\bar{r}}(k_z = 0) = \nu_{A(C);\bar{r}}(k_z = \pi) \bmod 2$ and $\nu_B(k_z = 0) \equiv \nu_B(k_z = \pi)$.

With these constraints in our hands, we can now analyze the flow of the corner charge Q_A as the momentum k_z completes an adiabatic cycle. The fourfold rotoinversion symmetry $\mathcal{S}_4$ ensures $Q_A(k_z) = -Q_A(-k_z) \bmod 1/2$, which is in agreement with the quantization of the corner charge in multiples of one quarter of the electronic charge in the planes $k_z = 0$ and $k_z = \pi$ [34]. As a result, we can only distinguish between two "topologically" distinct states. In fact, for $Q_A(0) = Q_A(\pi) \bmod 1$, the flow of the corner charge as k_z makes an adiabatic cycle that will be qualitatively similar to Fig. 3(b), and the hinges of the three-dimensional crystal will host an even number of chiral states. On the contrary, for $Q_A(0) = Q_A(\pi) \pm 1/2 \bmod 1$, and similarly to Fig. 3(a), an odd number of chiral hinge states will cross the Fermi level, thereby leading to a pattern of chiral hinge modes schematically shown in Fig. 4(b). Therefore, the difference in the integer invariants $\nu_{A;\bar{r}}$ at $k_z = 0, \pi$ provides the bulk $\mathbb{Z}_2$ topological invariants for a fourfold rotoinversion symmetry-protected second-order topological insulator.

Two remarks are in order here. First, the difference between the integer invariants $\nu_{C;\bar{r}}$ at $k_z = 0, \pi$ equals the difference in the A invariants, thereby implying the existence of a single $\mathbb{Z}_2$ bulk topological invariant [38]. Second, contrary to the example of an inversion-symmetric Chern insulator where the crystalline symmetry only provides us with a criterion for the Chern number parity [39,40], here the fourfold rotoinversion $\mathcal{S}_4$ represents the fundamental symmetry protecting the presence of chiral hinge states. It therefore plays the same stabilizing role time-reversal symmetry plays in two- and three-dimensional topological insulators in class AII.

We finally corroborate our findings by considering a tight-binding model corresponding to a three-dimensional stack of the two-dimensional crystal shown Fig. 1(a). The layers are connected by purely imaginary hoppings $\pm it_4$, as well as real diagonal next-nearest-neighbor hoppings t_5 [cf. Fig. 4(a)]. Note that these interlayer hoppings break separately the $\mathcal{C}_4$ and $\mathcal{M}_z$ symmetries, but respect their combination. Finally, we have included a π flux threading each plaquette surrounding the Wyckoff positions A, B, C, and D. At half filling, a direct computation of the two-dimensional crystalline invariants using Eq. (2) on the $k_z = 0, \pi$ planes [cf. Fig. 4(c)] yields $\nu_{A;\bar{r}}(k_z = 0) = 2 \bmod 4$ and $\nu_{A;\bar{r}}(k_z = \pi) = 0 \bmod 4$ [see Fig. 4(c)]. Our $\mathbb{Z}_2$ topological criterion then predicts the presence of chiral hinge states when considering the system in an open geometry. This is precisely what we find by diagonalizing the corresponding Hamiltonian with open boundary conditions in the $\hat{x}$ and $\hat{y}$ direction: Two chiral hinge states going upwards and two chiral hinge states going downwards transverse the bulk band gap of the system [see Fig. 4(d)], in perfect agreement with the hinge mode pattern shown in Fig. 4(b).

Conclusions. To sum up, we have characterized the bulk topology of second-order topological insulators with anomalous chiral hinge modes protected by inversion and rotoinversion symmetries. The corresponding bulk $\mathbb{Z}_2$ topological invariant, defined in terms of the occupied symmetric hybrid Wannier functions, can be equally expressed using the crystalline symmetry labels in the bulk band-structure representation. Therefore, our invariant can be straightforwardly computed by not only using tight-binding models but also in density functional theory calculations where higher-order topological candidate materials can be identified. A promising future direction is to extend the methodology proposed in this Rapid Communication to time-reversal symmetric systems.

Acknowledgments. C.O. acknowledges support from a VIDI grant (Project No. 680-47-543) financed by the Netherlands Organization for Scientific Research (NWO). This work is part of the research programme of the Foundation for Fundamental Research on Matter (FOM), which is part of the Netherlands Organization for Scientific Research (NWO).

[1] N. Marzari and D. Vanderbilt, Phys. Rev. B **56**, 12847 (1997).
[2] N. Marzari, A. A. Mostofi, J. R. Yates, I. Souza, and D. Vanderbilt, Rev. Mod. Phys. **84**, 1419 (2012).
[3] R. Sakuma, Phys. Rev. B **87**, 235109 (2013).
[4] B. Bradlyn, L. Elcoro, J. Cano, M. G. Vergniory, Z. Wang, C. Felser, M. I. Aroyo, and B. A. Bernevig, Nature (London) **547**, 298 (2017).
[5] H. C. Po, A. Vishwanath, and H. Watanabe, Nat. Commun. **8**, 50 (2017).
[6] M. Z. Hasan and C. L. Kane, Rev. Mod. Phys. **82**, 3045 (2010).
[7] X.-L. Qi and S.-C. Zhang, Rev. Mod. Phys. **83**, 1057 (2011).
[8] A. A. Soluyanov and D. Vanderbilt, Phys. Rev. B **83**, 035108 (2011).
[9] S. Coh and D. Vanderbilt, Phys. Rev. Lett. **102**, 107603 (2009).

[10] T. L. Hughes, E. Prodan, and B. A. Bernevig, Phys. Rev. B **83**, 245132 (2011).

[11] G. van Miert, C. Ortix, and C. M. Smith, 2D Mater. **4**, 015023 (2016).

[12] J.-W. Rhim, J. Behrends, and J. H. Bardarson, Phys. Rev. B **95**, 035421 (2017).

[13] G. van Miert and C. Ortix, Phys. Rev. B **96**, 235130 (2017).

[14] M. Sitte, A. Rosch, E. Altman, and L. Fritz, Phys. Rev. Lett. **108**, 126807 (2012).

[15] J. Langbehn, Y. Peng, L. Trifunovic, F. von Oppen, and P. W. Brouwer, Phys. Rev. Lett. **119**, 246401 (2017).

[16] Z. Song, Z. Fang, and C. Fang, Phys. Rev. Lett. **119**, 246402 (2017).

[17] M. Ezawa, Phys. Rev. Lett. **120**, 026801 (2018).

[18] F. Schindler, A. M. Cook, M. G. Vergniory, Z. Wang, S. S. Parkin, B. A. Bernevig, and T. Neupert, Sci. Adv. **4**, eaat0346 (2018).

[19] M. Geier, L. Trifunovic, M. Hoskam, and P. W. Brouwer, Phys. Rev. B **97**, 205135 (2018).

[20] E. Khalaf, Phys. Rev. B **97**, 205136 (2018).

[21] C. Fang and L. Fu, arXiv:1709.01929.

[22] F. Schindler, Z. Wang, M. G. Vergniory, A. M. Cook, A. Murani, S. Sengupta, A. Y. Kasumov, R. Deblock, S. Jeon, I. Drozdov, H. Bouchiat, S. Guéron, A. Yazdani, B. A. Bernevig, and T. Neupert, Nat Phys., doi:10.1038/s41567-018-0224-7 (2018).

[23] M. Ezawa, Phys. Rev. B **97**, 155305 (2018).

[24] M. Ezawa, Phys. Rev. B **97**, 241402(R) (2018).

[25] W. A. Benalcazar, J. C. Y. Teo, and T. L. Hughes, Phys. Rev. B **89**, 224503 (2014).

[26] J. Kruthoff, J. de Boer, J. van Wezel, C. L. Kane, and R.-J. Slager, Phys. Rev. X **7**, 041069 (2017).

[27] Y. Zhou, K. M. Rabe, and D. Vanderbilt, Phys. Rev. B **92**, 041102 (2015).

[28] W. A. Benalcazar, B. A. Bernevig, and T. L. Hughes, Science **357**, 61 (2017).

[29] W. A. Benalcazar, B. A. Bernevig, and T. L. Hughes, Phys. Rev. B **96**, 245115 (2017).

[30] Y. Xu, R. Xue, and S. Wan, arXiv:1711.09202.

[31] M. Serra-Garcia, V. Peri, R. Süsstrunk, O. R. Bilal, T. Larsen, L. G. Villanueva, and S. D. Huber, Nature (London) **555**, 342 (2018).

[32] C. W. Peterson, W. A. Benalcazar, T. L. Hughes, and G. Bahl, Nature (London) **555**, 346 (2018).

[33] S. Imhof, C. Berger, F. Bayer, J. Brehm, L. Molenkamp, T. Kiessling, F. Schindler, C. H. Lee, M. Greiter, T. Neupert, and R. Thomale, arXiv:1708.03647.

[34] See Supplemental Material at http://link.aps.org/supplemental/10.1103/PhysRevB.98.081110 for a detailed derivation of the integer topological invariants in $\mathcal{C}_2, \mathcal{C}_3, \mathcal{C}_6$ rotational-symmetric two-dimensional crystals and for second-order topological insulators in $\mathcal{C}_2 \times \mathcal{M}_z \equiv \mathcal{I}$ and $\mathcal{C}_6 \times \mathcal{M}_z \equiv \mathcal{C}_3 + \mathcal{I}$ three-dimensional crystals.

[35] Since the Wyckoff positions B and D are transformed into each other by a fourfold rotation $N_{B;\pm1} \equiv N_{D;\pm1}$.

[36] The $\mathbb{Z}^8$ topological classification for the space group $p4$ reported in Ref. [24] considers the total number of occupied bands as an additional integer topological invariant.

[37] The topological classification presented for $\mathcal{C}_4$-symmetric crystals applies equally to $\mathcal{C}_4 \times \mathcal{M}_z$-symmetric 2D crystals.

[38] The $\mathcal{S}_4$ symmetry ensures $N_A(k_z) + N_C(k_z) + 2N_B(k_z) = N_F$ for $k_z = 0, \pi$, where $N_W(k_z) = \sum_r N_{W;r}(k_z)$. It follows that $N_A(\pi) - N_A(0) = N_C(0) - N_C(\pi) + 2[N_B(0) - N_B(\pi)]$. Since $\nu_B(\pi) = \nu_B(0)$, we find $N_B(\pi) = N_B(0) \bmod 2$. This in turn implies $\nu_{A,\bar{r}}(\pi) - \nu_{A,\bar{r}}(0) = \nu_{C,\bar{r}}(\pi) - \nu_{C,\bar{r}}(0) \bmod 4$, where we have used that $N_{A(C)}(k_z = 0, \pi) = \nu_{A(C);\bar{r}}(k_z = 0, \pi) \bmod 4$.

[39] A. M. Turner, Y. Zhang, R. S. K. Mong, and A. Vishwanath, Phys. Rev. B **85**, 165120 (2012).

[40] C. Fang, M. J. Gilbert, and B. A. Bernevig, Phys. Rev. B **86**, 115112 (2012).